Supporting Information

Interplay of Defect and dopant in *l*-Dopa aided UiO-66 for Superprotonic Conductivity

Powrnika Selvakumar,[a] Sathish Kumar Somu,[a] Sri Vanaja Swaminathan,[a] Amrita Pal,[b] Aneesh Anand Nechikott,[a] Prashant Kumar Nayak,[a] Tanay Kundu[a]*

[a]Department of Chemistry, SRM Institute of Science and Technology, Kattankulathur, Tamil Nadu, India

[b]Department of Chemistry, Sathyabama Institute of Science and Technology, Jeppiaar Nagar, Rajiv Gandhi Salai, Chennai - 600 119, Tamil Nadu, India

***Author for correspondence (tanayk@srmist.edu.in)**

Table of Contents

S1. Synthesis of LD@D-UiO-66

The Ratios of *l*-Dopa and 1,4-BDC in different batches of high-throughput synthesis are given below.

BATCH	*l*-DOPA%	1,4-BDC%
D-UiO-66	0	100
1	15	85
2	20	80
3	25	75
4	30	70
5	35	65
6	40	60
7	45	55
8	50	50
9	100	0

Table. S1 Ratios of *l*-Dopa and 1,4-BDC in different batches of high-throughput synthesis

S2. UV-DRS and Tauc plot

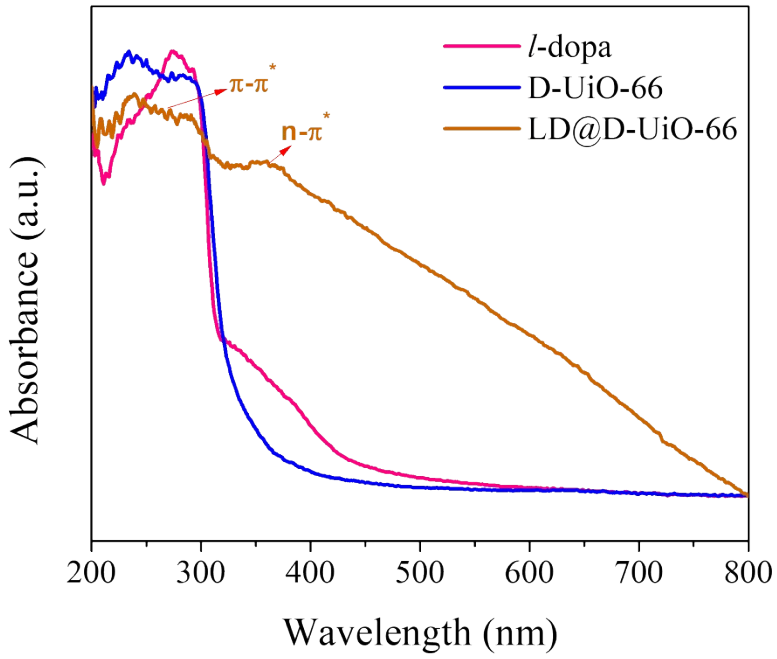

Figure S1. UV-DRS of *l*-Dopa, D-UiO-66 and LD@D-UiO-66

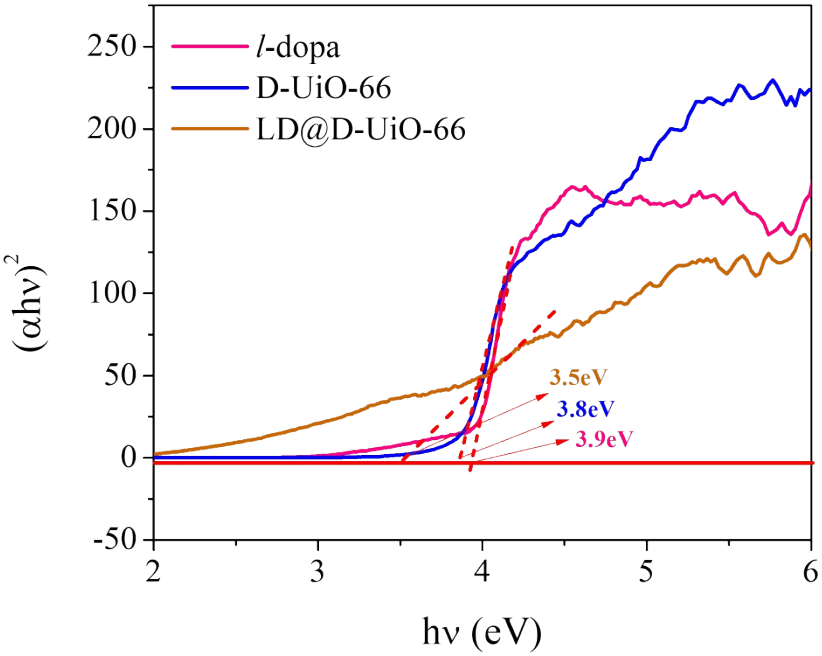

Figure S2. Tauc plot of *l*-Dopa, D-UiO-66 and LD@D-UiO-66

S3. Thermogravimetric analysis (TGA)

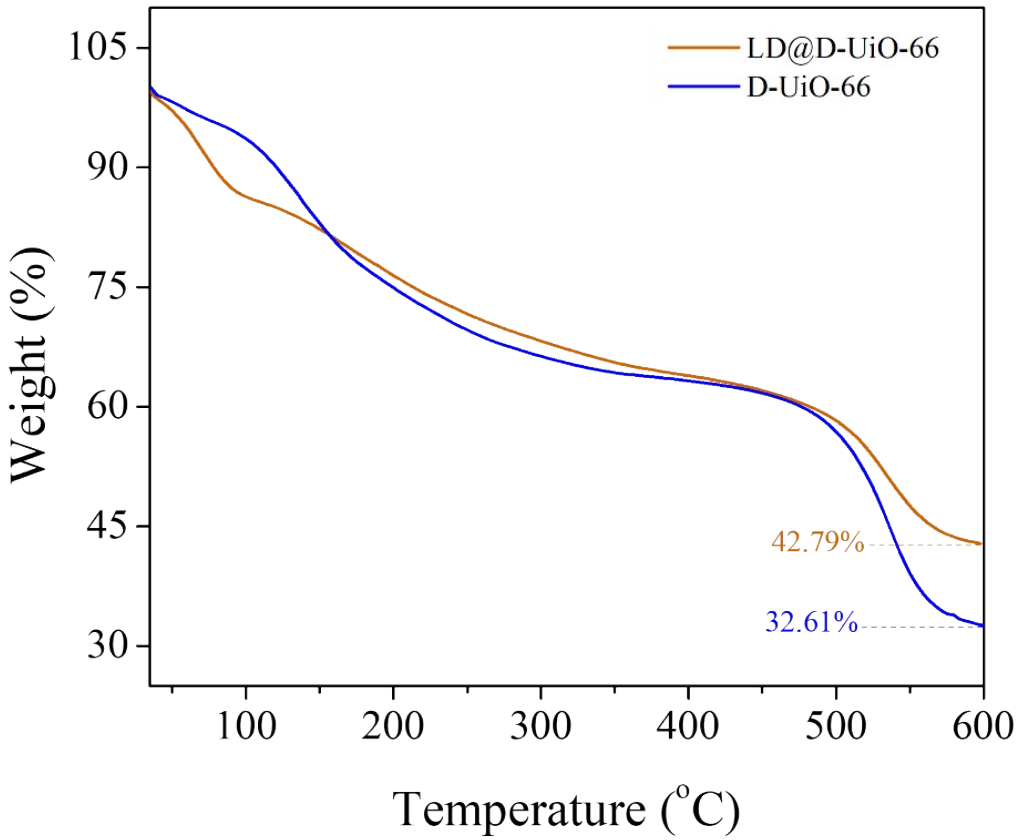

Figure S3. TGA of D-UiO-66 and LD@D-UiO-66

S4. PXRD, FTIR-Before and after Proton conductivity studies

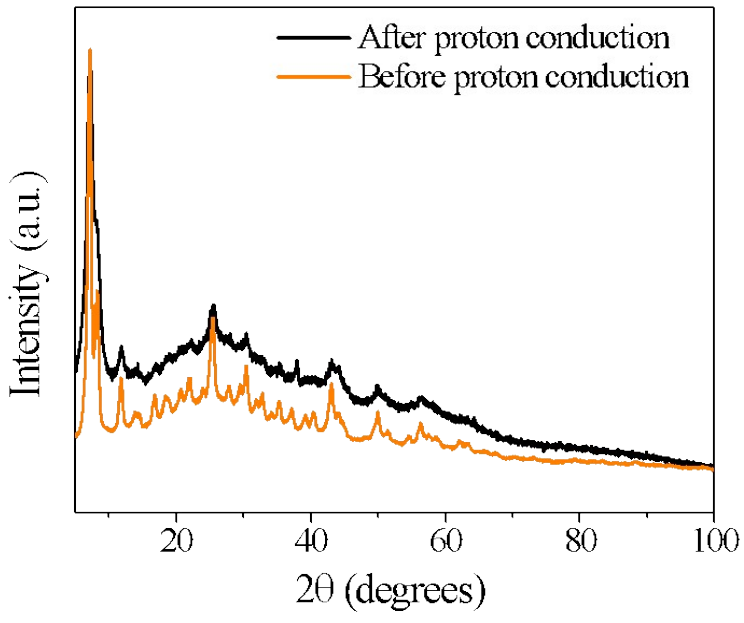

Figure S4. PXRD patterns of LD@D-UiO-66 before and after proton conductivity measurements

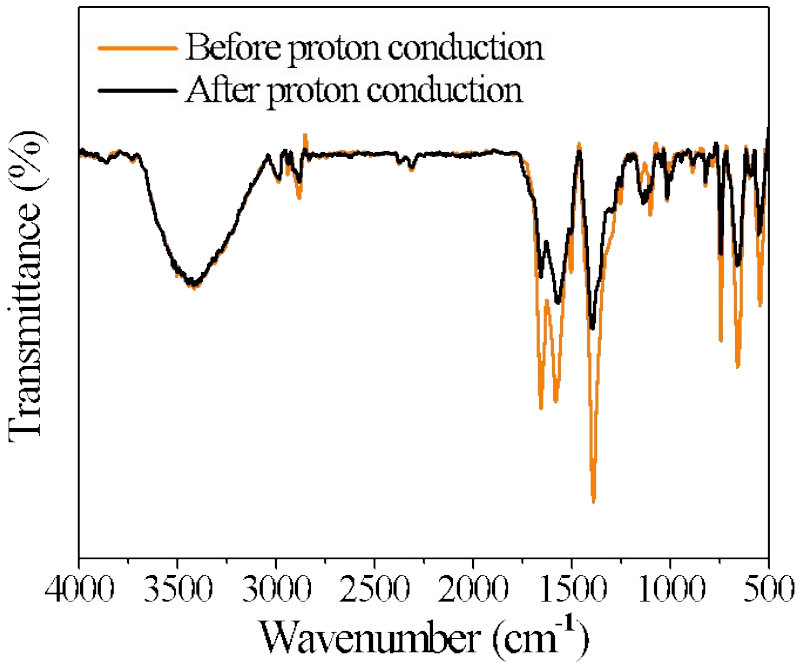

Figure S5. FTIR spectra of LD@D-UiO-66 before and after proton conductivity measurements

From the PXRD pattern (Fig. S4) and FTIR spectrum (Fig. S5) it is evident that the structural integrity before and after proton conduction is preserved.

S5. X-ray Photoelectron Spectroscopy (XPS) and the elemental compositions of D-UiO-66, LD@D-UiO-66, and *l*-Dopa

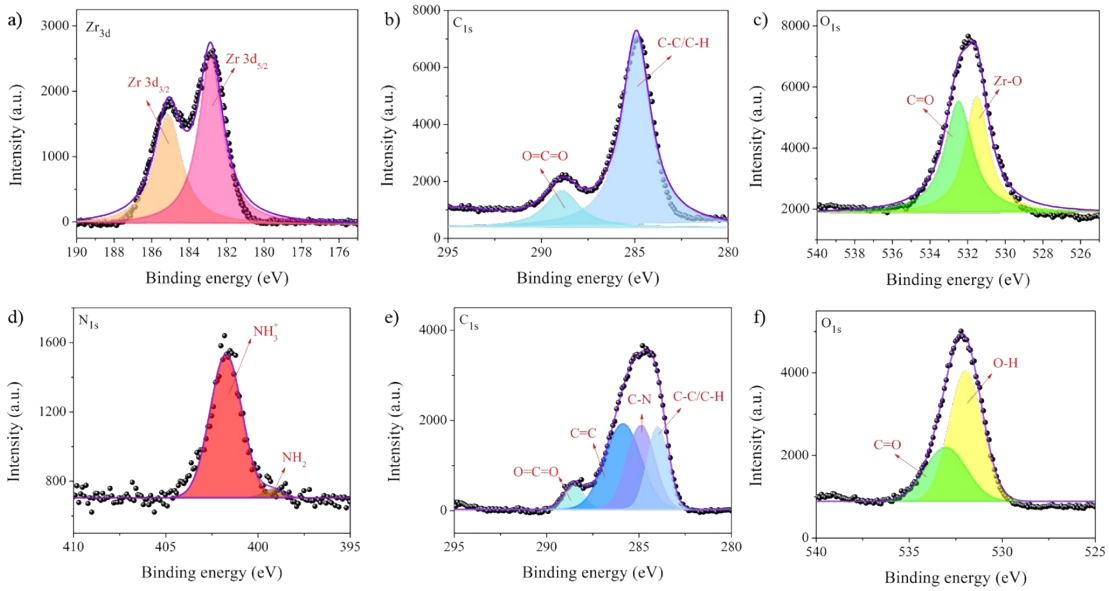

Figure S6. a) Zr 3d of D-UiO-66. b) C 1s of D-UiO-66 c) O 1s of D-UiO-66. d) N 1s of *l*-Dopa. e) C 1s of *l*-Dopa. f) O 1s of *l*-Dopa

LD@D-UiO-66	**Zr 3d**	**C 1s**	**N 1s**	**O 1s**
	3.49%	66.35%	0.68%	29.49%
D-UiO-66	**Zr 3d**	**C 1s**	**N 1s**	**O 1s**
	3.90%	66.59%	Insignificant	29.47

Table S2. Percentage of elemental compositions of D-UiO-66, LD@D-UiO-66.

Zr 3d	**D-UiO-66**	**LD@D-UiO-66**
Zr 3d 5/2	182.85 eV	182.82 eV
Zr 3d 3/2	185.12 eV	185.21 eV
C 1s	**D-UiO-66**	**LD@D-UiO-66**
C-C/CH	284.52 eV	284.73 eV

C-N	-	285.66 eV
C=C	-	286.68 eV
O=C=O	288.96 eV	288.75 eV
O 1s	**D-UiO-66**	**LD@D-UiO-66**
Zr-O	531.48 eV	531.56 eV
C=O	532.46 eV	532. 36 eV
N 1s	**D-UiO-66**	**LD@D-UiO-66**
NH_3^+	-	400.46 eV

Table S3. Binding energies of D-UiO-66, LD@D-UiO-66.

S6. Calculation of percentage of missing linkers per Zr_6

From the help of XPS, we obtained the ratio of Zr:C:O in the samples and the calculation is as follows. Considering the ratio of C:O, using the formula

$$\textbf{Defect\%} = (1-(C_{calc}/C_{obs}))*100$$

for D-UiO-66, we got Defect%=33.6%. And, for LD@D-UiO-66, Defect%=31.7%. The number of missing linkers per Zr_6 in both D-UiO-66 and LD@D-UiO-66 is approximately 2.

Sample	**Zr:C:O**	**Defect%**	**Number of linkers present per Zr_6**	**Number of missing linkers per Zr_6**
Pristine UiO-66	1:8:5.33	Nil	6	Nil
D-UiO-66	1:17.074:7.556	33.6%	3.98	6-3.98=2.02 ≈ 2
LD@D-UiO-66	1:16.318:7.418	31.7%	4.08	6-4.08=1.92 ≈ 2

Table S4. Calculation of percentage of missing linkers per Zr_6

S7. Proton conductivity calculation

T (°C)	**T (K)**	**Resistance(Ω)**	**ln (σT)**	**1000/T (K^{-1})**	**Proton conductivity (S cm^{-1})**

25	298.15	210.92	-1.862775	3.354016435	5.2E-04
30	303.15	191.2	-1.747985	3.298697015	5.7E-04
40	313.15	126.36	-1.301346	3.193357816	8.7E-04
50	323.15	62.457	-0.565255	3.09453814	1.8E-03
60	333.15	31.64	0.145278	3.001650908	3.5E-03
70	343.15	18.04	0.736683	2.914177473	6.1E-03
80	353.15	8.4	1.529768	2.831657936	1.3E-02
90	363.15	6.89661	1.754893	2.753683051	**1.6E-02**

Table S5. Proton conductivity calculation for D-UiO-66

T (°C)	T (K)	Resistance(Ω)	ln (σT)	1000/T (K^{-1})	Proton conductivity (S cm^{-1})
25	298.15	72	-0.7908	3.354016	1.5E-03
30	303.15	58	-0.5551	3.298697	1.9E-03
40	313.15	30	0.1313	3.193358	3.6E-03
50	323.15	26	0.2947	3.094538	4.2E-03
60	333.15	16	0.8431	3.001651	7.0E-03
70	343.15	11	1.2209	2.914177	9.9E-03
80	353.15	7	1.7477	2.831658	1.6E-02
90	363.15	5	2.0298	2.753683	**2.1E-02**

Table S6. Proton conductivity calculation for LD@D-UiO-66

S8. Nyquist plots

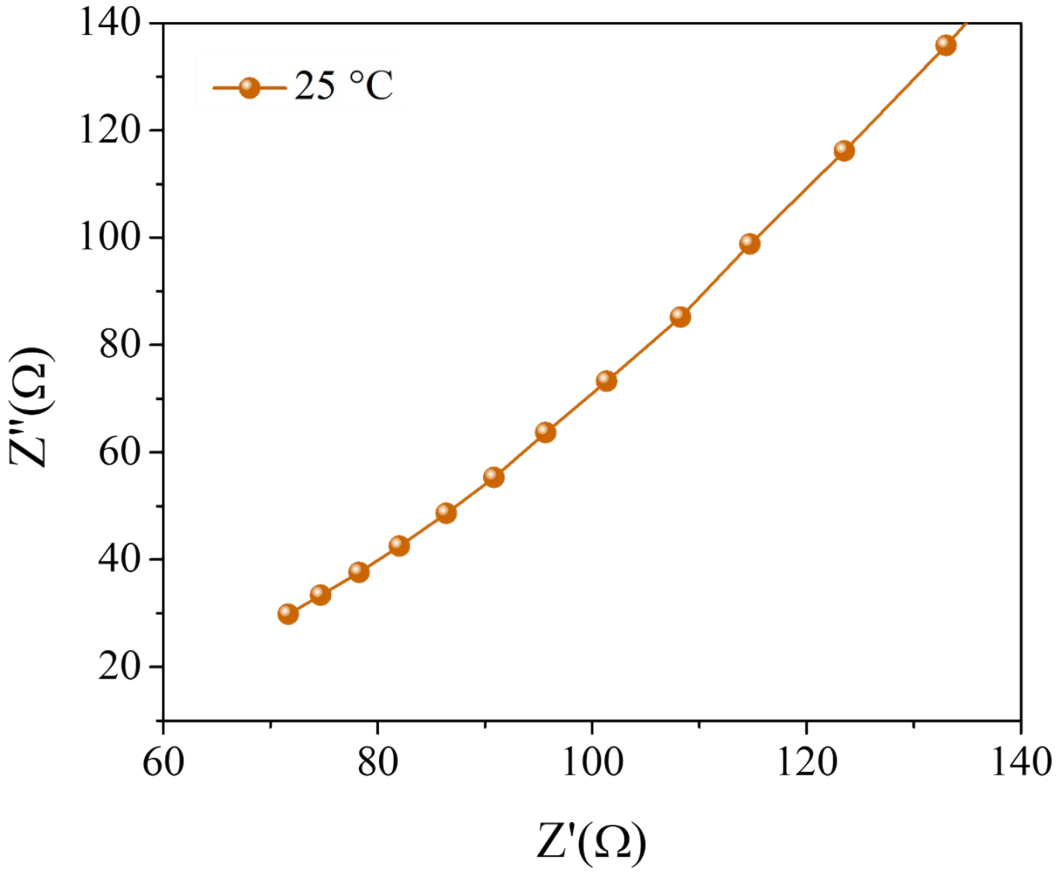

Figure S7. Nyquist plot indicating proton conductivity of LD@D-UiO-66 at room temperature (25 °C)

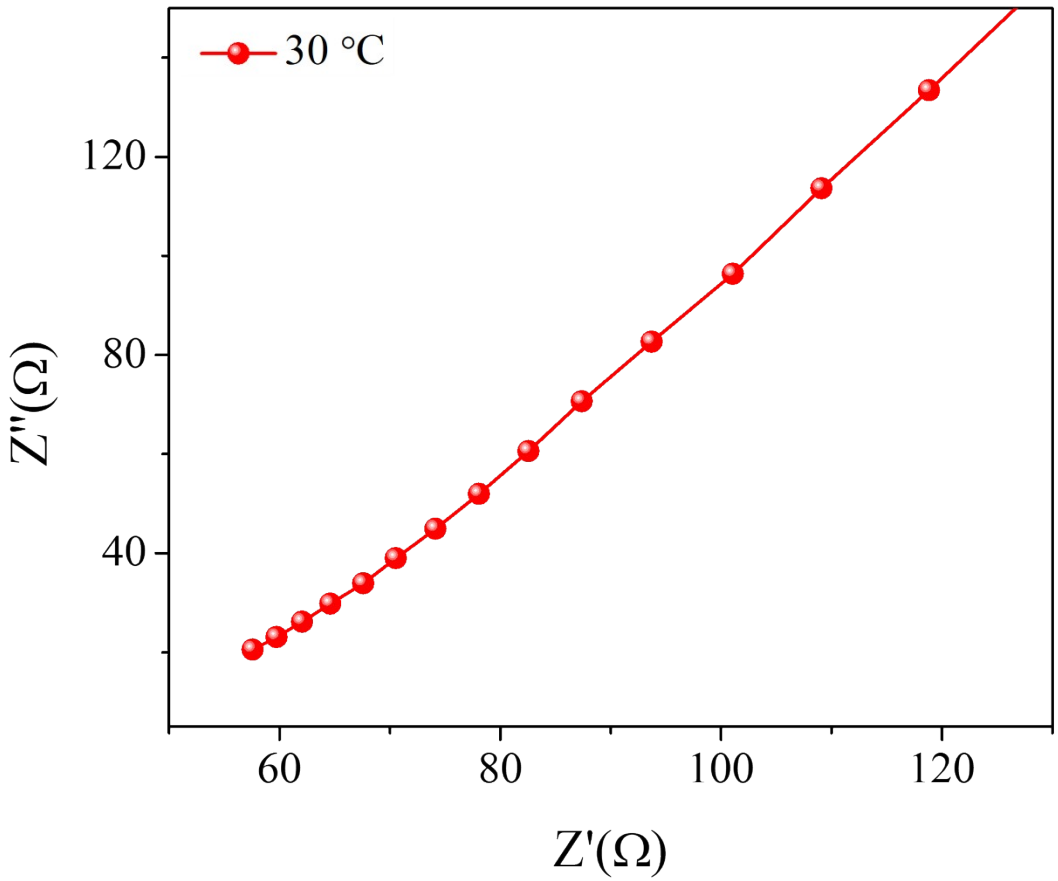

Figure S8. Nyquist plot indicating proton conductivity of LD@D-UiO-66 at 30 °C

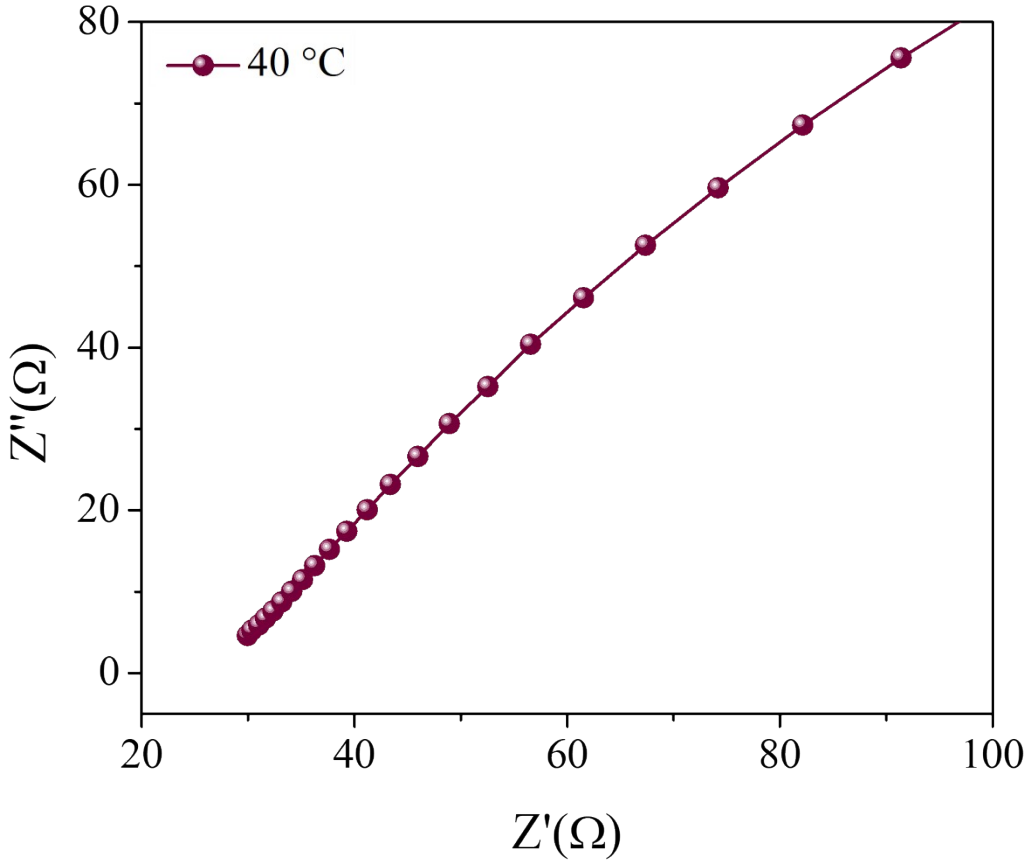

Figure S9. Nyquist plot indicating proton conductivity of LD@D-UiO-66 at 40 °C

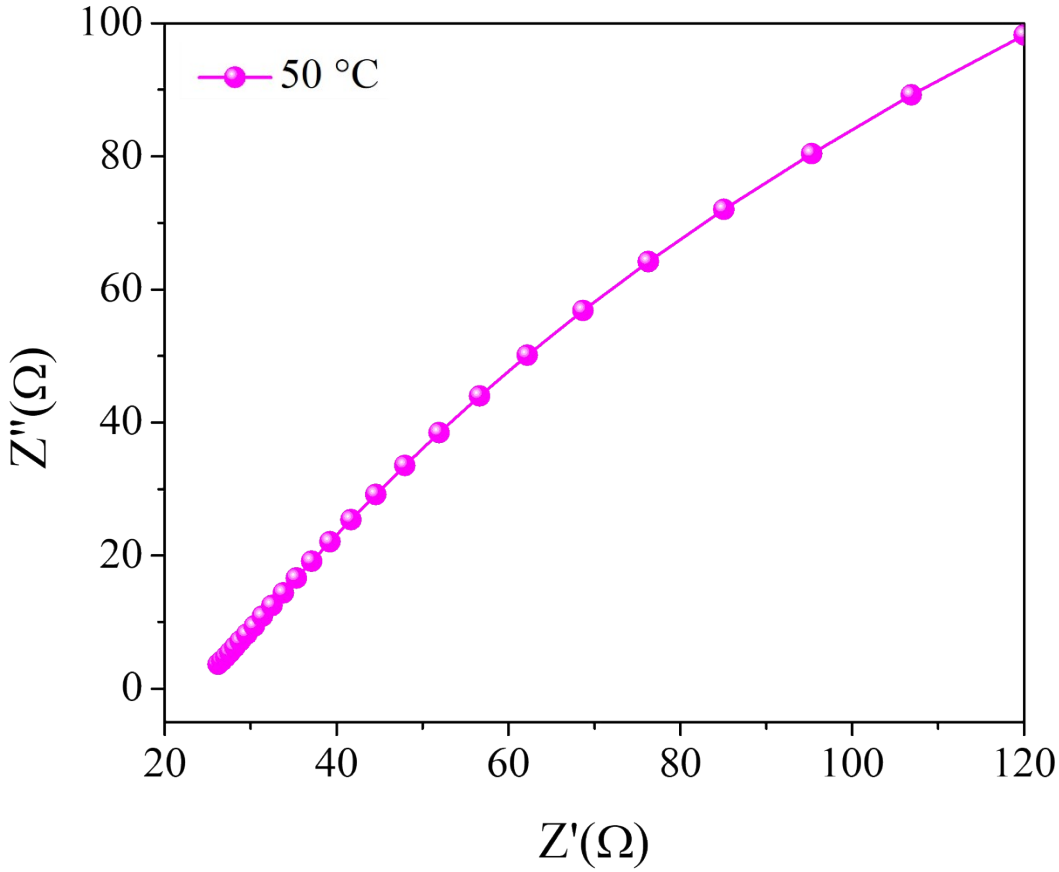

Figure S10. Nyquist plot indicating proton conductivity of LD@D-UiO-66 at 50 °C

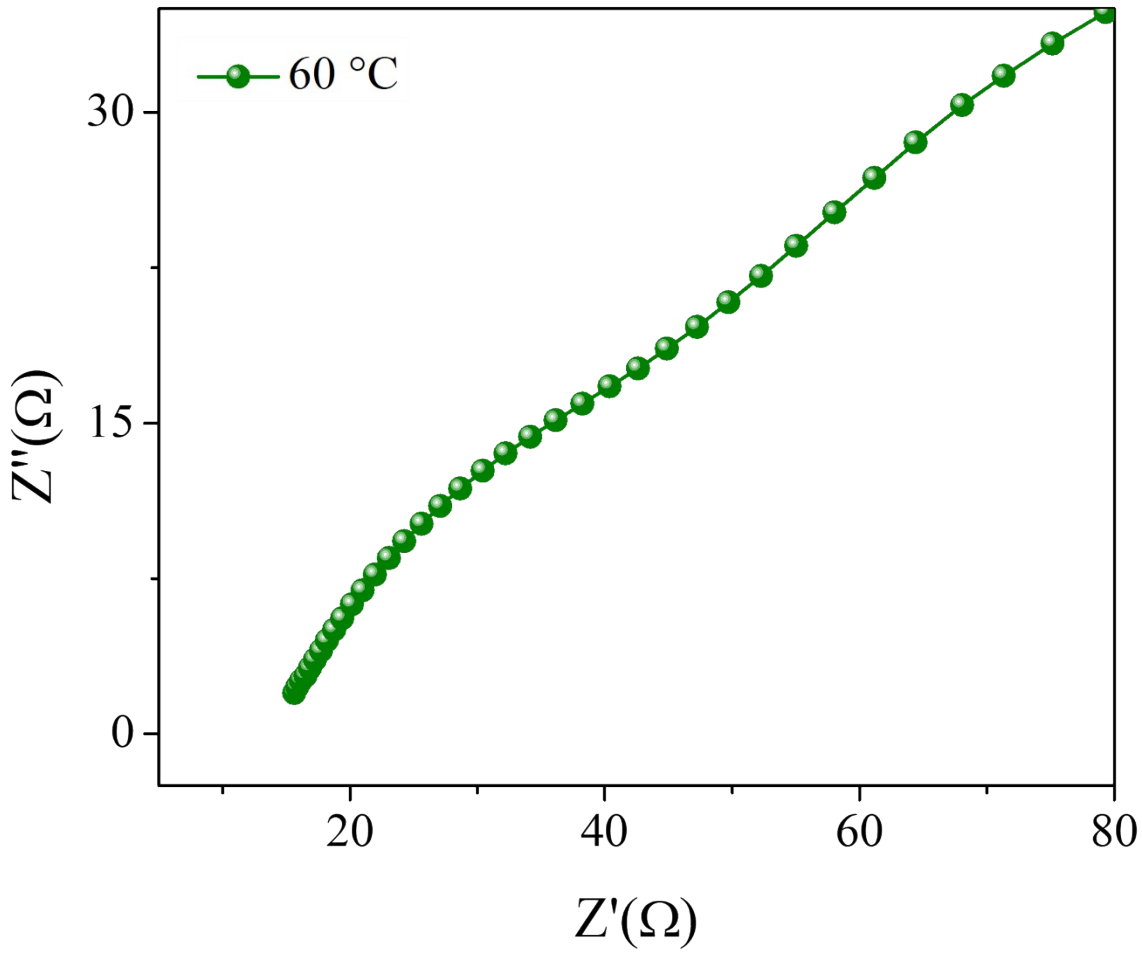

Figure S11. Nyquist plot indicating proton conductivity of LD@D-UiO-66 at 60 °C

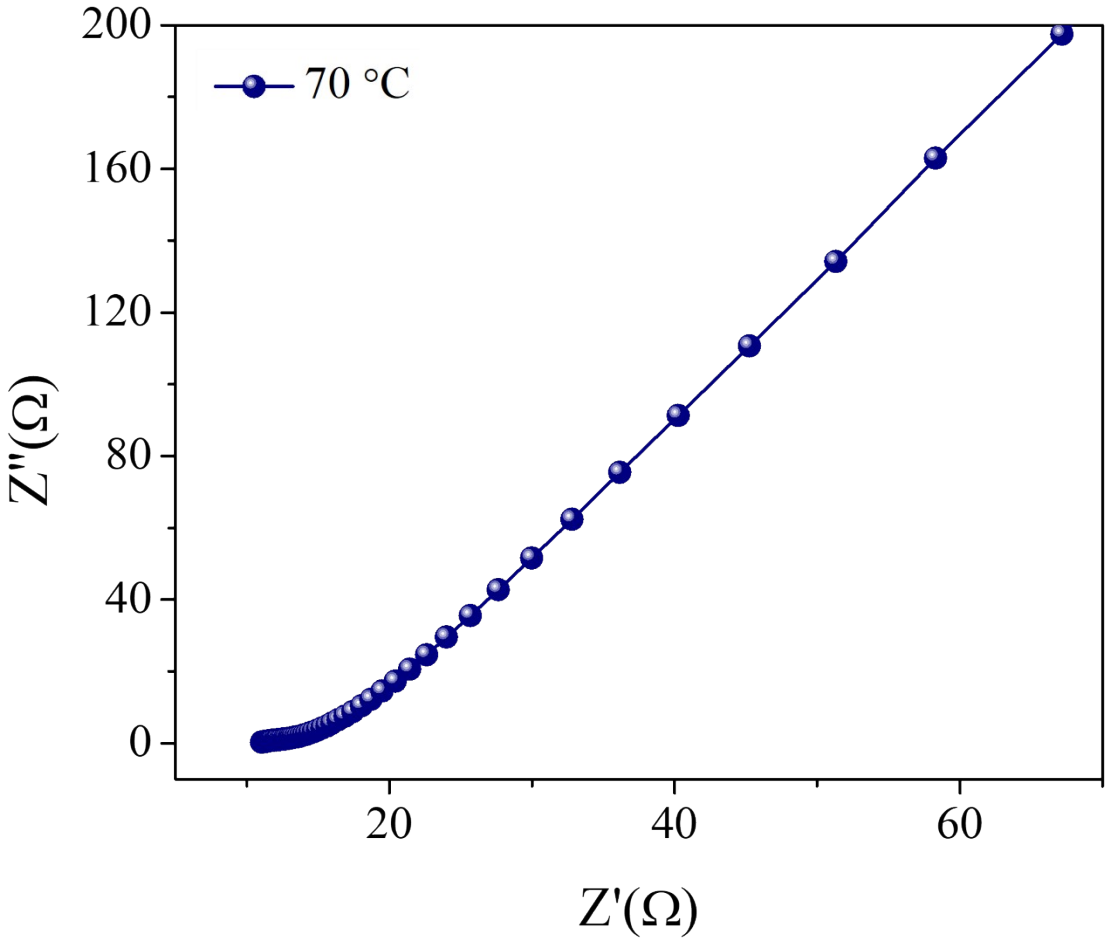

Figure S12. Nyquist plot indicating proton conductivity of LD@D-UiO-66 at 70 °C

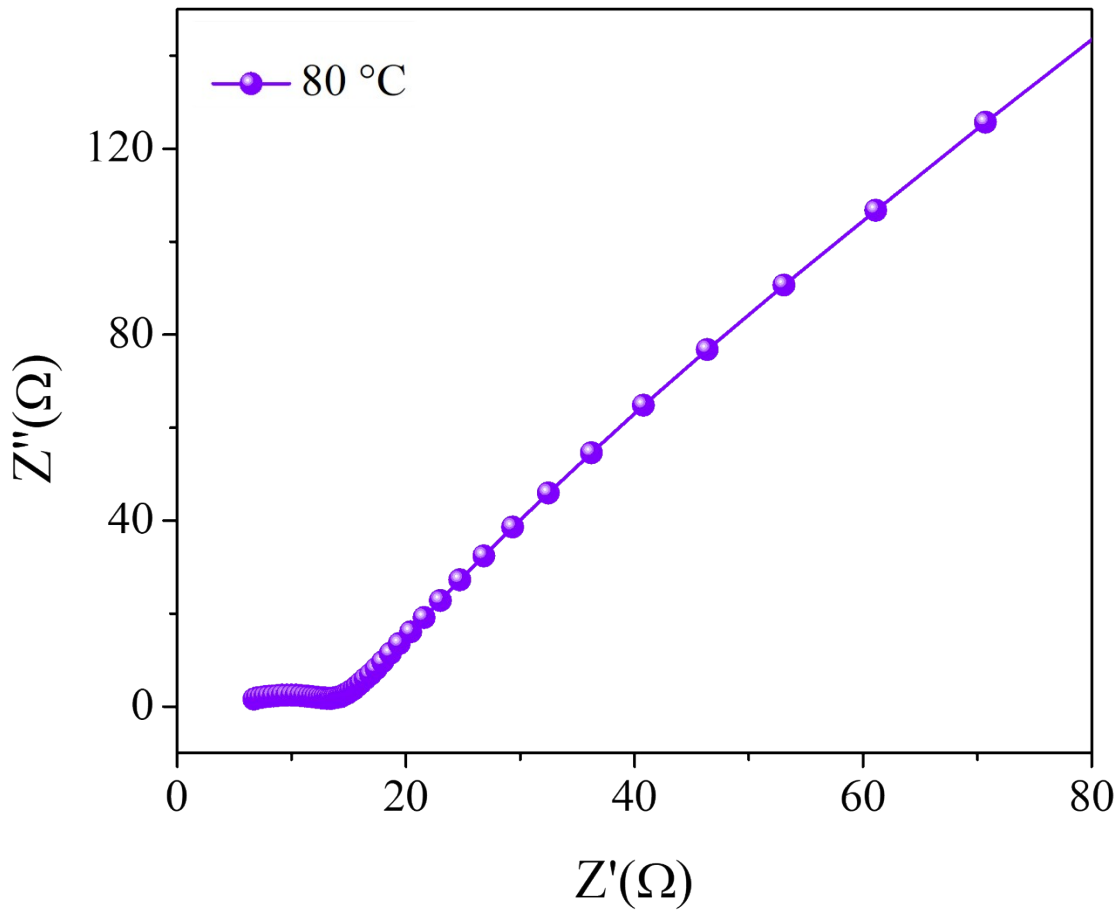

Figure S13. Nyquist plot indicating proton conductivity of LD@D-UiO-66 at 80 °C

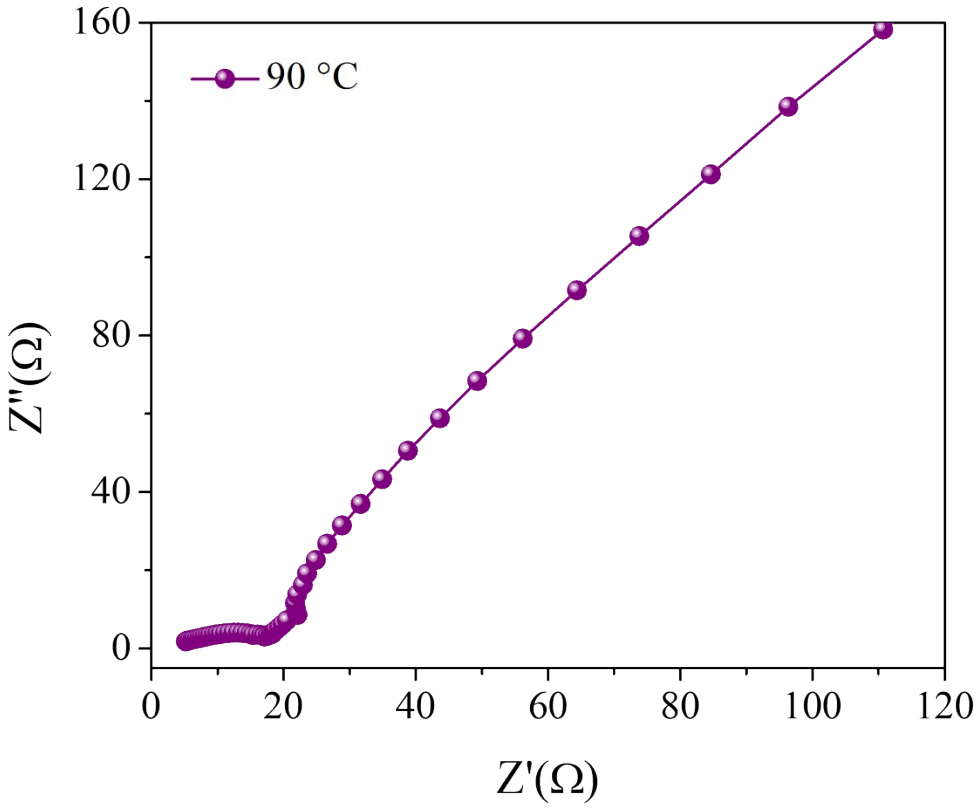

Figure S14. Nyquist plot indicating proton conductivity of LD@D-UiO-66 at 90 °C

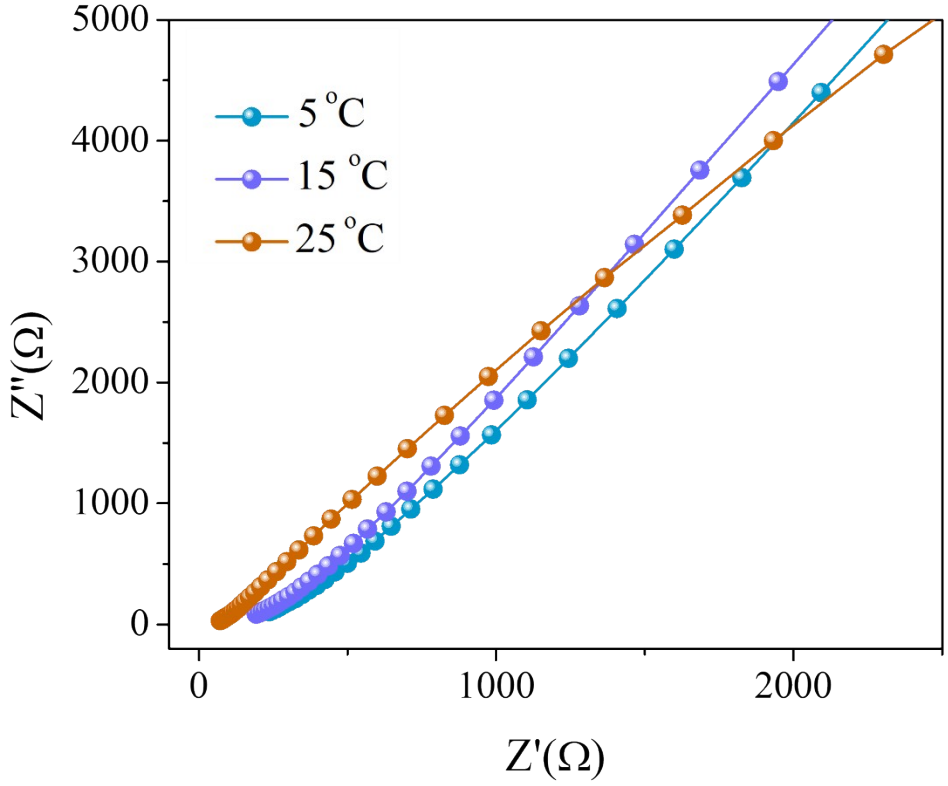

Figure S15. Nyquist plot indicating proton conductivity of LD@D-UiO-66 for the range of 5-25 °C.

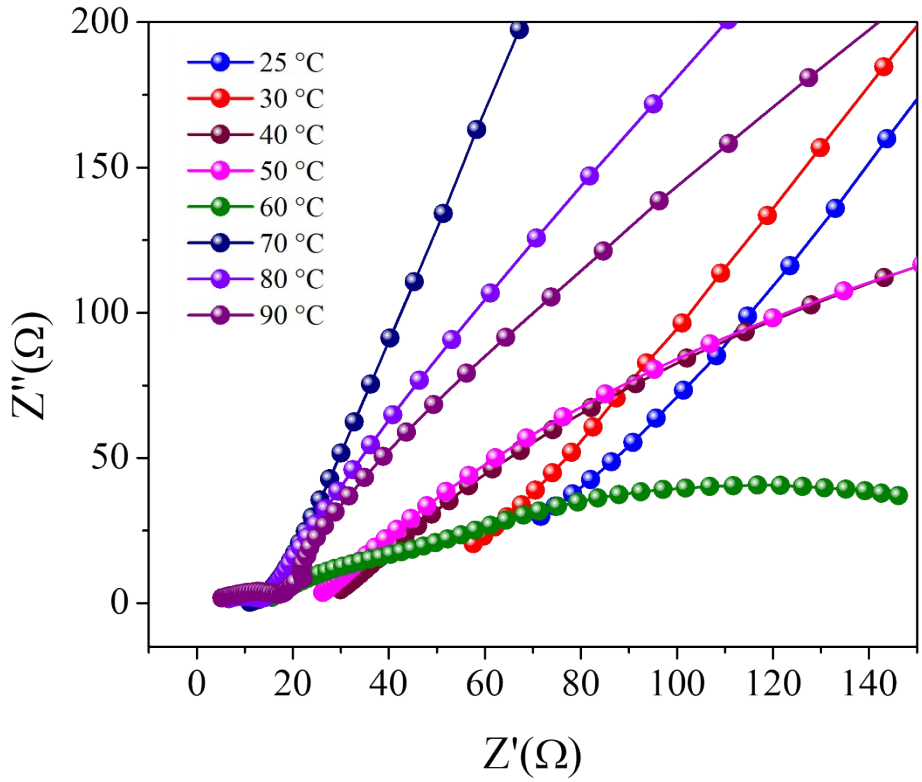

Figure S16. Nyquist plots indicating proton conductivity of D-UiO-66 for the temperature range from 25-90 °C.

S9. Activation energy calculation

Arrhenius plot data for D-UiO-66		
Temperature	**1000/T**	**Log (σT)**
25	3.354016435	-1.862775167
30	3.298697015	-1.747985236
40	3.193357816	-1.301345635
50	3.09453814	-0.565254676
60	3.001650908	0.145277728
70	2.914177473	0.736683187
80	2.831657936	1.529768222
90	2.753683051	1.754893017
Ea = -1(8.314*-6.51) = 54.12KJ/mol = 0.57ev		

Table S7. Activation energy calculation for D-UiO-66 at different temperature range

Arrhenius plot data for LD@D-UiO-66		
Temperature	**1000/T**	**Log (σT)**
25	3.354016435	-0.790776515
30	3.298697015	-0.555064312
40	3.193357816	0.131347464
50	3.09453814	0.294731449
60	3.001650908	0.843067574
70	2.914177473	1.220913179
80	2.831657936	1.747706648
90	2.753683051	2.02984581
Ea = -1(8.314*-4.6923) = 39.012KJ/mol = 0.40ev		

Table S8. Activation energy calculation for LD@D-UiO-66 at different temperature range

S10. Temperature vs proton conductivity

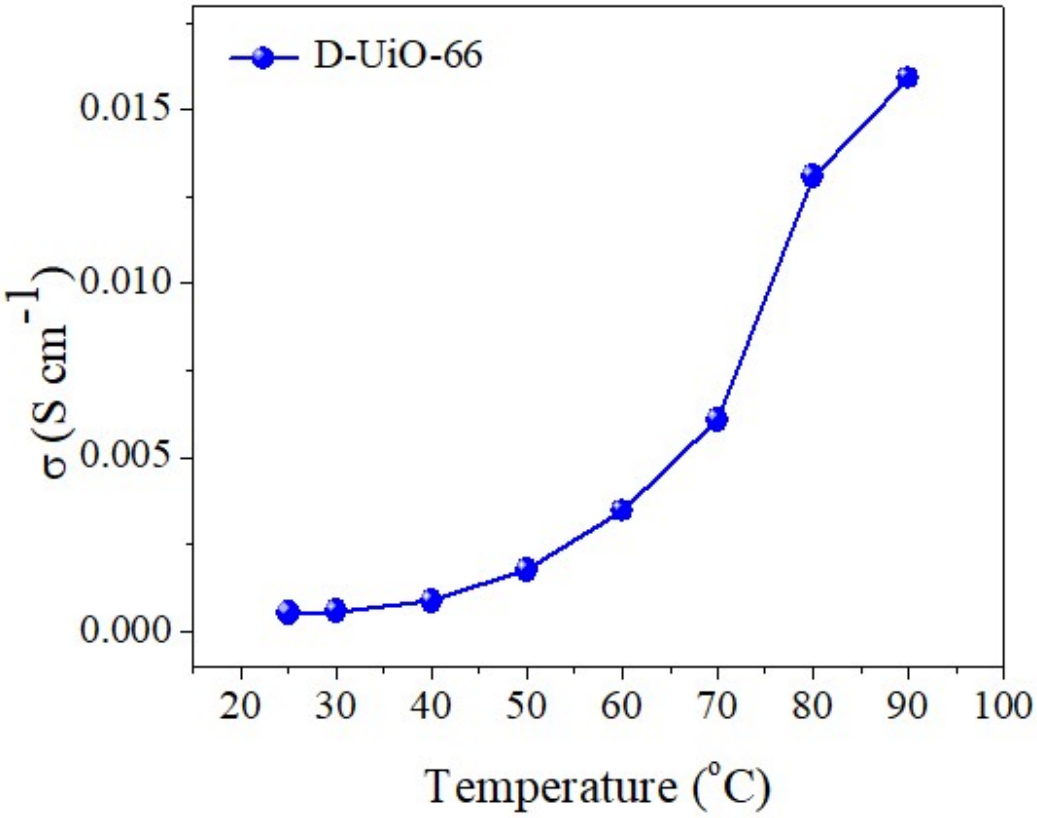

Figure S17. Temperature vs Proton Conduction plot for D-UiO-66.

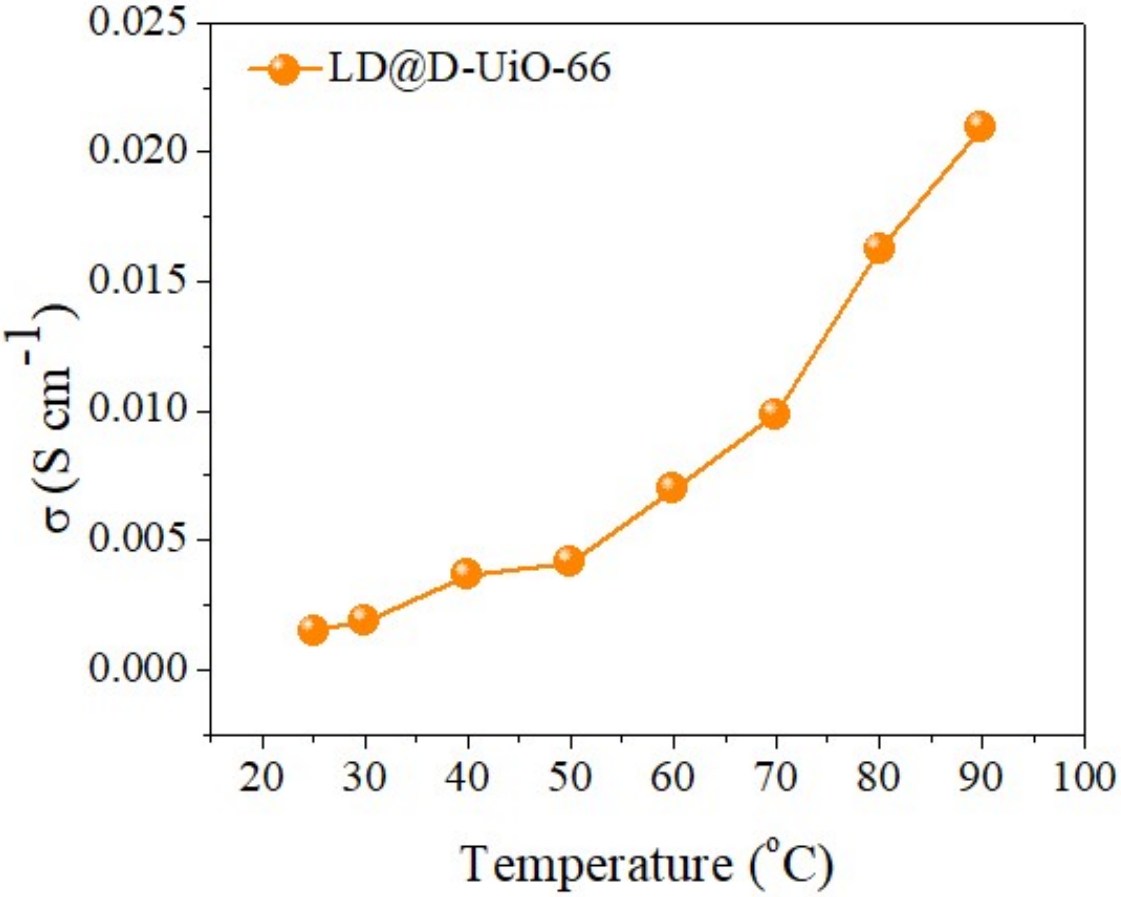

Figure S18. Proton Conduction vs Temperature plot for LD@D-UiO-66.

S11. Relative humidity vs proton conductivity at 25 °C

Relative Humidity (% RH)	Temperature (°C)	Resistance (Ω)	Proton conductivity (S cm^{-1})
42	25	720.8770752	1.5E-04
54	25	581.1678467	1.9E-04
62	25	454.3648682	2.4E-04
77	25	415.6928711	2.6E-04
84	25	278.6865234	3.9E-04
98	25	73.88426208	1.5E-03

Table S9. Relative Humidity vs Proton Conduction plot for LD@D-UiO-66.

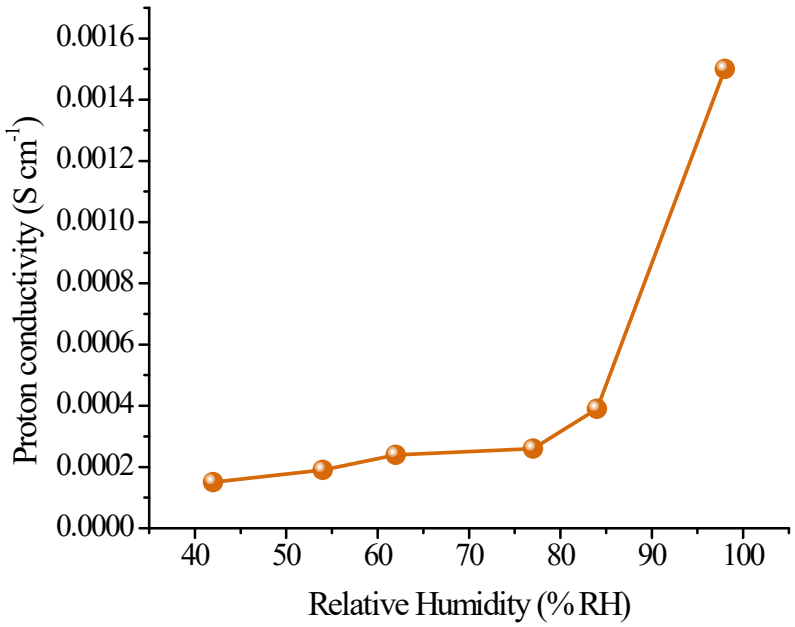

Figure S19. Relative Humidity vs Proton Conduction plot for LD@D-UiO-66.

S12. Comparison table of Nafion and LD@D-UiO-66

Key comparison factors	Nafion	LD@D-UiO-66
Cost	N117, N212, N424 cost varies over a range from $100-$1000 per square meter/sheet. So, per kg would cost much more than $1000.	LD@D-UiO-66 synthesized using pure chemicals cost around $787, lesser than $1000.
Environmental impact	Nafion polymer contain forever chemicals because of presence of C-F bonds, which contributes to global warming. Thermolysis of Nafion leaves perfluorinated backbone, which is a potential hazard to the environment.[1]	LD@D-UiO-66 is synthesized with sustainable, eco-friendly chemicals.
Proton conductivity	Around 6.5 to 98 mS cm^{-1} at 80 °C, 25-100% RH.[2]	1.5×10^{-3} to 2.1×10^{-2} S cm^{-1} for 25-90 °C, 98% RH.

Table S10. Comparison table of Nafion and LD@D-UiO-66

S13. Comparison table of proton conductivities of UiO-66 based MOFs with current work

S.No.	UiO-66 based MOF	σ (S cm^{-1})	Reference	
1	UiO-66-defects	6.79×10^{-3}	Taylor et al., *Chem. Mater.,* 2015	3
2	UiO-66-Hf	4.56×10^{-2}	Fang et al.,*CrystEngComm.,* 2015	4
3	Ce-UiO-66	1.24×10^{-1}	Wang et al., *Int. J. Hydrogen Energy.,* 2015	5
4	60-UiO-66-1.8	1.04×10^{-1}	Liu et al., *Inorg. Chem*., 2022	6
5	UiO-66-SO_3H	3.4×10^{-2}	Yang et al., *Crst. Growth Des*., 2015	7
6	**LD@D-UiO-66**	**2.1×10^{-2}**	**This work**	
7	D-UiO-66-N=IM	2.15×10^{-2}	Li et al., *Chem. Commun*., 2024	8
8	UiO-66=IM	4.18×10^{-2}	Tran et al., *Int. J. Hydrogen Energy.,* 2024	9
9	UiO-66-N=IM	7.48×10^{-4}	Li et al., *Chem. Commun*., 2024	8
10	D-UiO-66-NH_2	6.18×10^{-3}	Li et al., *Chem. Commun*., 2024	8
11	UiO-66-SO_3H/NH_2	3.78×10^{-3}	Zhang et al., *Int. J. Hydrogen Energy.,* 2024	10
12	UiO-66-2COOH	1.00×10^{-3}	Yang et al., *Crst. Growth Des*., 2015	7
13	UiO-66-SO_3H	3.4×10^{-3}	Yang et al., *Crst. Growth Des*., 2015	7
14	UiO-66$(SO_3H)_2$	8.4×10^{-2}	Zou et al., Inorg. Chem., 2021	11
15	Lys-UiO-66-$(COOH)_2$@CS-7	2.2×10^{-2}	Gao et al., Carbohydr. Polym., 2025	12
16	UiO-66-$(COOH)_2$@PVP/PVDF	5.76×10^{-3}	Gao et al., *Int. J. Hydrogen Energy.,* 2024	13
17	Pristine UiO-66	7.54×10^{-6}	Yang et al., *Cryst. Growth Des*., 2015	7

Table S11. Proton conductivities of UiO-66 based MOFs

S14. References

1. Feng, M., Qu, R., Wei, Z., Wang, L., Sun, P. and Wang, Z., *Sci. Rep.*, 2015, **5**, 9859.
2. Y. Kim, K. Ketpang, S. Jaritphun, J. S. Park and S. Shanmugam*, J. Mater. Chem. A,* 2015, **3**, 8148–8155.
3. J. M. Taylor, S. Dekura, R. Ikeda and H. Kitagawa, *Chem. Mater.*, 2015, **27**, 2286–2289.
4. F. Fang, P. Wang, Z. Zhang, S. S. Zhang, Y. Y. Guo, S. Y. Wang, L. Du and Q. H. Zhao, *CrystEngComm*, 2024, **26**, 2751–2754.
5. Q. Wang, D. Shen, Z. Tu and S. Li, *Int. J. Hydrogen Energy*, 2024, **56**, 1249–1256.
6. Q. Q. Liu, S. S. Liu, X. F. Liu, X. J. Xu, X. Y. Dong, H. J. Zhang and S. Q. Zang, *Inorg. Chem.*, 2022, **61**, 3406–3411.
7. F. Yang, H. Huang, X. Wang, F. Li, Y. Gong, C. Zhong and J. R. Li, *Cryst. Growth Des.*, 2015, **15**, 5827–5833.
8. X. M. Li, J. Jia, M. Zhao, D. Liu, J. Gao and Y. Q. Lan, *Chem. Commun.,* 2024, **60**, 6777–6780.
9. M. H. Tran, L. C. Jheng, Z. L. Zhao, W. C. Ko, K. S. Ho and T. C. Liao, *Int. J. Hydrogen Energy*, 2024, **77**, 1375–1386.
10. X. Zhang, J. Long, M. Wang, Y. Liu and H. Ma, *Int. J. Hydrogen Energy*, 2024, 61, 1495–1504.
11. X. N. Zou, D. Zhang, Y. Xie, T. X. Luan, W. Li, L. Li and P. Z. Li, *Inorg. Chem.*, 2021, **60**, 10089–10094.
12. Y. Gao, P. He, J. Yang, B. Liu, Q. Zhang, Q. Zhou, H. Xu, R. Jiang, Z. Dai and S. Wang, *Carbohydr. Polym.*, 2025, **348**, 122835
13. Gao, Y.; Zhou, Q.; Xu, H.; Liu, B.; Zhang, Q.; Dai, Z.; Wang, S.; Jiang, R, *Chem. Commun.,* 2024, **60***,* 6777–6780.